

Numerical estimates for the spectrum of quantum chromodynamics

Herbert Hamber

Brookhaven National Laboratory, Upton, New York, 11973

Giorgio Parisi

*Istituto di Fisica della Facoltà di Ingegneria, Università degli Studi, Roma, Italy
and Istituto Nazionale di Fisica Nucleare, Frascati, Italy*

(Received 13 May 1982)

We present estimates for the hadron masses in lattice QCD obtained in the approximation of neglecting dynamic-fermion loops. Both light- and heavy-quark systems are considered and their dependence on the coupling constant and the quark mass is studied. Some results for the decay amplitudes are also given. We discuss how the η' mass can be computed to lowest order in n_f , the number of dynamic fermion flavors.

I. INTRODUCTION

Recently some numerical estimates for the particle spectrum of lattice gauge theories¹ have been obtained using an approximation in which the effects of dynamic-fermion loops are neglected.²⁻⁵ This corresponds to setting n_f , the number of fermion flavors, equal to zero in the fermionic contribution to the probability measure used in generating gauge-field configurations by Monte Carlo methods.⁶ From this point of view the method has the advantage of not having to include in the statistical factor the determinant of the Dirac operator (a highly nonlocal object) which arises once the fermion degrees of freedom are integrated out. Although several viable techniques have been suggested for including, at least in an approximate way, the effects of the determinant,⁷⁻¹⁴ they still seem to require perhaps an order of magnitude more computing time than a local bosonic action would imply. Typically the bosonic update requires matrix element of fermionic operators which are themselves computed by a stochastic method with diverging relaxation times in the small-quark-mass limit.

On the other hand the inclusion of fermion-loop effects has been studied in two-dimensional gauge theories, where it can be shown that, at least for some quantities, like the average plaquette energy or the fermion propagator at the origin, the feedback changes indeed very little.^{10,12} Simulations in four-dimensional QCD tend to confirm this picture. In this case the approximation is justified in the large- N_c limit (where fermion loops are suppressed by a factor of $1/N_c$ with respect to gluon loops), and arguments can be given for the smallness of these effects for finite $N=3$ both at weak ($g_0 \ll 1$) and strong ($g_0 \gg 1$) coupling. Indeed if one excludes

special cases like the η' mass, which is believed to arise mostly because of the anomaly induced in the isoscalar axial-vector current by the presence of fermion-annihilation diagrams,¹⁵ one might expect that the inclusion of these effects would change hadron-mass estimates only by a few percent. Phenomenological considerations can also be given in support of this statement. It is conceivable that for the heavier hadrons the inclusion of the loops will mostly reflect itself into a readjustment of the unphysical length scale a (the lattice spacing), leaving most mass ratios unchanged.

The plan of the paper is as follows. In Sec. II we define our notation for the lattice action and remind the reader of the different ways in which the Dirac operator can be transcribed on the lattice, and discuss briefly the advantages and drawbacks of the various formulations. The two options that we consider are Wilson's form for the action,¹ which is known to avoid the problem of fermion species doubling both at weak and strong coupling at the price of breaking chiral symmetry completely in the massless case, and the Kogut-Susskind-type form,¹⁶⁻¹⁸ which preserves a chiral symmetry but introduces four flavors on the lattice for each flavor in the continuum theory. Since we actually have, in our approximation, zero flavors we have still avoided a full confrontation with the doubling problem.

A brief description is then given of how to compute meson and baryon propagators on a finite lattice and the importance of cutoff-dependent corrections to the continuum-theory results. We will obtain masses and amplitudes by looking at the large-distance falloff of the propagator, or, equivalently, its small-momentum behavior.

Our estimates for the hadron spectrum of QCD (limited to flavor nonsinglets) are presented in Secs.

III and IV. We have now considerably increased the statistics and have analyzed 393 independent gauge-field configurations, to be compared with the 50 configurations of our earlier work, Ref. 2. Also results on larger lattices (up to $6^3 \times 12$ sites) are included. We have three parameters that we can vary: the bare coupling constant g_0 , the quark mass m , and the size of the lattice. In order to verify that we are actually computing physical quantities in the continuum theory, we have studied their dependence on the coupling g_0 and found agreement with the scaling behavior predicted by the renormalization group. (In Ref. 2 we did not follow the renormalization-group behavior of the masses as a function of g_0^2 , since we limited ourselves to $g_0^2=1$.) Since our cutoffs (proportional to a^{-1}) vary (exponentially) with the bare coupling, changing the latter corresponds to exploring different mass regions in the spectrum. Thus for stronger couplings we obtain estimates for the lighter hadrons (π , ρ , p , . . .), whereas for weaker coupling we move into the region of charmed states ($\eta_c, J/\psi$, . . .).

We will consider in detail the pseudoscalar (0^{-+}), vector (1^{-}), scalar (0^{++}), axial-vector (1^{++}), and tensor (1^{+-}) mesons, some of their lowest radial excitations, and the $\frac{1}{2}^{+}$ and $\frac{3}{2}^{+}$ baryon states. The only parameters we have to use as input in our calculation are the lattice spacing at a particular value of g_0 (it sets the absolute scale for the masses), as determined, e.g., from the Regge slope or the ρ - π mass difference, and the quark mass (m_u , m_d , m_s , . . .). Since this last quantity is not known from experiment, we will trade it for a physical mass like the pion mass, and from the latter estimate the quark masses.

In Sec. IV we will give our results for the decay amplitudes, which can be extracted from the meson propagators. The amplitudes can then be used to estimate, for example, leptonic decay widths.

Finally in the last section we show how to compute the mass of the η' to lowest order in n_f ,

without having to include the effects of dynamic-fermion loops in the simulation.

II. DESCRIPTION OF THE METHOD

We will write the lattice QCD action (for one fermion flavor) as^{1,19-22}

$$\begin{aligned} S &= S_G + S_F, \\ S_G &= \frac{1}{2g_0^2} \sum_{n,\mu,\nu \neq \mu} \text{Tr}(U_{n\mu} U_{n+\mu,\nu} U_{n+\nu,\mu}^\dagger U_{n\nu}^\dagger), \\ S_F &= k \sum_{n,\mu} \bar{\psi}_n [(r - \gamma_\mu) U_{n\mu} \psi_{n+\mu} \\ &\quad + (r + \gamma_\mu) U_{n-\mu,\mu}^\dagger \psi_{n-\mu}] \\ &\quad - \sum_n \bar{\psi}_n \psi_n. \end{aligned} \quad (2.1)$$

Here S_G is the pure gauge action, g_0 is the bare coupling constant, and the $U_{n\mu}$'s are 3×3 complex matrices, elements of the group SU(3). S_F is the fermion action with four-component spinors $\bar{\psi}, \psi$. It depends on a parameter r that interpolates between Wilson ($r=1$) and Kogut-Susskind-type ($r=0$) fermions, and on a hopping constant k (in general different for different flavors) related to the bare quark mass by

$$m = \ln[1 + \frac{1}{2}(1/k - 1/k_c)] \quad (2.2)$$

and $k_c = \frac{1}{8}$ for $g_0=0$ (free fermions) and $r=1$, whereas for $r=0$ the fermion mass is

$$m = 1/2k. \quad (2.3)$$

The continuum Dirac fields and related to the above lattice fields by

$$\psi_{\text{cont}}(na) = (2k/a^3)^{1/2} \psi_n. \quad (2.4)$$

It is instructive to look at the free-fermion propagator obtained from S_F (with $U=1$),

$$\langle \bar{\psi}_n \psi_0 \rangle = a^4 \int_{-\pi/a}^{\pi/a} \frac{d^4 p}{(2\pi)^4} \frac{e^{i p a n}}{1 - 2ik \sum_{\mu} \gamma_{\mu} \sin p_{\mu} a - 2kr \sum_{\mu} \cos p_{\mu} a}. \quad (2.5)$$

For $r=1$ (in fact for any $r \neq 0$) there is no symmetry that prevents k_c from getting renormalized^{1,16-23} but the dependence of k_c on g_0 is not known except around $g_0=0$ ($k_c = \frac{1}{8}$) and $g_0 = \infty$, ($k_c \simeq \frac{1}{4}$). In this formulation one has, in order to approach the massless limit, to adjust k so as to at least partially cancel the mass term with the r -dependent counterterm. In this formulation the chiral-symmetry-breaking

terms are of order $(pa)^2$ for small pa , and give important contributions only for momenta of the order of the cutoff. We therefore expect reliable estimates of large-distance behavior of correlation functions (determined by the pole in momentum space) as opposed to more local quantities like $\langle \bar{\psi} \psi \rangle$, the fermion propagator at the origin, which should at least require a subtraction.

For $r=0$ the theory has a full chiral symmetry, but is known to describe 16 flavors instead of 1.^{16,17} By an appropriate canonical transformation the flavors can be reduced to four, maintaining at the same time the invariance of the theory under a set of chiral symmetries. One sets²⁰

$$\begin{aligned}\psi_n &= T_n \chi_n, \\ \bar{\psi}_n &= \bar{\chi}_n T_n^\dagger, \\ T_n &= (\gamma_1)^{n_x} (\gamma_2)^{n_y} (\gamma_3)^{n_z} (\gamma_4)^{n_t}.\end{aligned}\quad (2.6)$$

The fermionic action then becomes (after rescaling the fields by $\sqrt{2k}$)

$$S_F = \sum_n \bar{\psi}_n [(D_x \psi)_n + (-)^{n_x} (D_y \psi)_n + (-)^{n_x + n_y} (D_z \psi)_n + (-)^{n_x + n_y + n_z} (D_t \psi)_n + m \psi_n], \quad (2.7)$$

where D_μ is the covariant version of the central first derivative ∂_μ . In this framework there is no problem in computing a local quantity like $\langle \bar{\psi} \psi \rangle$, but, because of the increased lattice periodicity ($2a$ instead of a), in the case of the staggered fermions a larger lattice in the “time” direction is required in order to extract masses from the exponential decay

$$\begin{aligned}\langle \bar{\psi}(0) \Gamma \psi(0) \rangle &= \int d\mu[A] \text{Tr}[\Gamma G(0,0;A)], \\ \langle \bar{\psi}(x) \Gamma \psi(x) \bar{\psi}(0) \Gamma \psi(0) \rangle &= \int d\mu[A] \text{Tr}[G(x,0;A) \Gamma G(0,x;A) \Gamma], \\ \langle \bar{\psi}(x) \bar{\psi}(x) \bar{\psi}(x) \psi(0) \psi(0) \psi(0) \rangle &= \int d\mu[A] \text{Tr}[G(x,0;A) G(x,0;A) G(x,0;A)],\end{aligned}\quad (2.9)$$

where we have suppressed flavor, spinor, and color indices, Γ is a γ matrix (in the case of the Kogut-Susskind fermions it is a suitable linear combination of factors $(-)^n$, the components of n being either zero or one) and $G(x,0;A)$ is the inverse of $\mathcal{D} + m$ in a background A_μ gauge-field configuration. For operators that do have the flavor quantum numbers of the vacuum (i.e., $J=S=B=0$) additional contributions to the propagator are present in the form

$$\int d\mu[A] \text{Tr}[G(x,x;A) \Gamma G(0,0;A) \Gamma]. \quad (2.10)$$

The propagator $G(x,0;A)$ can be computed using the Monte Carlo (MC) method [some care is needed since $\mathcal{D} + m$ is not a positive-definite operator; a suitable action is $||(\mathcal{D} + m)\phi||^2$], the Langevin equation or the relaxation method. When using the relaxation method to compute correlation functions^{2-5,10,12} one has to solve the equation

$$(\mathcal{D} + m)G(x,0;A) = \delta(x). \quad (2.11)$$

In the Langevin approach^{2,3,24} one writes down the equations

of the correlation functions. The separation of operators with different spin-parities seems also slightly more cumbersome in this formulation, especially for baryons.

Since $\bar{\psi}$ and ψ are anticommuting variables, they are not suited for numerical simulations. After integrating them out we get an effective probability measure for the gauge fields

$$d\mu[U] = e^{S_G} [\det(\mathcal{D} + m)]^{n_f} dU_H, \quad (2.8)$$

where $\mathcal{D} + m$ is the lattice Dirac operator and dU_H is the Haar measure for the group $SU(3)$. The effects of the fermion determinant can be included in a Monte Carlo simulation by using the methods of Ref. 7. Since the procedure is rather time consuming, we choose to set as a first approximation $n_f = 0^{2-5}$. In this way the feedback of the fermion dynamics on the gauge-field configuration is ignored.

Once a set of gauge-field configurations have been generated, e.g., by the Metropolis Monte Carlo method,^{1,6} $\langle \bar{\psi} \psi \rangle$ and the correlation functions of composite operators that do not have the flavor quantum numbers of the vacuum are computed by averaging appropriate fermionic Green's functions,

$$\begin{aligned}\partial_t \phi(x,t) &= [(-)^i \mathcal{D} + m] \phi_i(x,t) + \eta(x,t), \\ & i = 1, 2,\end{aligned}\quad (2.12)$$

where η is a Gaussian stochastic white noise

$$\langle \langle \eta(x,t) \eta(x',t') \rangle \rangle = 2\delta(t-t') \delta(x-x')$$

and the average $\langle \langle \rangle \rangle$ is over the noise. One then obtains

$$\lim_{t \rightarrow \infty} \langle \langle \phi_1(x,t) \phi_2^*(y,t) \rangle \rangle = G(x,y;A). \quad (2.13)$$

The stochastic methods (MC and Langevin) are particularly useful for local quantities because of their speed, whereas the relaxation method has some advantage when computing the large-distance behavior of correlation functions since it does not superimpose intrinsic fluctuations on the gauge-field variations. Typically the calculation of the fermion propagator with one source point fixed to a precision which is at worst one percent takes an amount of time comparable to several hundred MC sweeps.

As was done in Refs. 2-5 it is actually convenient

to define a new correlation function obtained by summing over space positions. Define

$$M_{\Gamma}(x,0) = \langle \bar{\psi}(x)\Gamma\psi(x)\bar{\psi}(0)\Gamma\psi(0) \rangle. \quad (2.14)$$

Then the propagator

$$\tilde{M}_{\Gamma}(t,0) = \sum_{\vec{x}} M_{\Gamma}(\vec{x},t;0) \quad (2.15)$$

projects out the zero-momentum state, and the large-time behavior is given by

$$\tilde{M}_{\Gamma}(t,0) \underset{t \rightarrow \infty}{\simeq} A e^{-mt}, \quad (2.16)$$

where m is the mass of the lowest state that is created from the vacuum by the operator $\bar{\psi}\Gamma\psi$. For t not too large one expects that additional higher-mass states that can be excited from the vacuum by the operator $\bar{\psi}\Gamma\psi$ will contribute subdominant corrections

$$\tilde{M}_{\Gamma}(t,0) \simeq \sum_n A_n e^{-m_n t}. \quad (2.17)$$

We will exploit this circumstance to compute radial excitations of the mesons.

Because of the periodic boundary conditions imposed on the system the behavior of the correlation functions \tilde{M}_{Γ} on a lattice of extent L in the time direction is expected to be of the form

$$\tilde{M}_{\Gamma}(t,0) \simeq A e^{-mt} + A e^{-m(L-t)} + \dots \quad (2.18)$$

We will take these corrections into account when we estimate masses.

To generate the gauge-field configurations we used the Metropolis Monte Carlo method^{1,6} with ten hits per site. Between 3000 and 4000 MC sweeps were used to allow for the system to reach thermal equilibrium. The size of the lattice was $5 \times 5 \times 5 \times 8$ in most cases, and $6 \times 6 \times 6 \times 10$ and $6 \times 6 \times 6 \times 12$ in a few cases, except for four checks on the masses done on a $4 \times 4 \times 4 \times 6$ lattice. The large size of the lattice in the time direction was necessary in order to separate the uninteresting short-distance perturbative contribution ($x^{-\text{integer}}$) from the large-distance exponential decay, and also to decrease the effective temperature ($T=1/L_t$) of the system. In each run the meson and baryon correlation functions were averaged over several (6–10) configurations separated by mostly 100 MC sweeps. Both ordered and disordered starting configurations were used at the three values of β ($\beta=6/g_0^2$) explored in more detail ($\beta=5.6, 6.0,$ and 6.4). At each value of β we used between three and four completely statistically independent configurations (in Ref. 2 we had only used one starting configuration, on which, then, successive MC iterations were performed). In part this was done in order to reduce the statistical correlations present between successive configurations in

the same MC run, which we found surprisingly to be rather strong, accounting for 10–20% systematic effects on the masses. When using the relaxation method the source point was chosen at random and the number of relaxation iterations was 100/500. Typically the correlation function $G(x,0;A)$ was evaluated to a relative precision of one part in 10^3 at the midpoint ($t=L_t/2$) or better in the mass region we have explored (with the exception of the points at $\beta=6.0, k=0.1525$ where the convergence is somewhat less accurate). For small fermion masses [$m_{\pi} \lesssim 3/S$, where S is the spatial or transverse extension of the lattice, $m \lesssim 0.1$, or $(k-k_c)/k_c \lesssim 5 \times 10^{-2}$] the relaxation method starts to converge more and more slowly and fluctuations in the density of eigenvalues of the matrix $\mathcal{D}+m$ become increasingly important. (See discussion in the next section). We have therefore tried to limit ourselves to a region of masses where the fluctuations are still contained.

III. HADRON-MASS ESTIMATES

We will now present our results. In the case of the Wilson fermions we have computed the masses of the (flavor-nonsinglet) pseudoscalar ($\Gamma=\gamma_5, J^{PC}=0^{-+}$), vector ($\gamma_{\mu}, 1^{--}$), scalar ($1, 0^{++}$), axial-vector ($\gamma_5 \gamma_{\mu}, 1^{+-}$), and tensor ($\sigma_{\mu\nu}, 1^{+-}$) meson states and of the $\frac{1}{2}^{+}$ (octet) and $\frac{3}{2}^{+}$ (decouplet) baryon states, as a function of $\beta=6/g_0^2$ and k (or m). The number of (almost) independent gauge-field configurations in each case is shown in Tables II–IV for each (β, k) . For small quark mass an increasing number of configurations is needed in order to get reliable estimates of the masses. This is because correlations within a gauge-field configuration become increasingly important. The qualitative behavior of $k_c(\beta)$ as obtained by studying a $2 \times 2 \times 2 \times 4$ lattice is shown in Fig. 1. K_c is determined by the vanishing of the pion mass or the appearance of a zero eigenvalue in $\mathcal{D}+m$. At $\beta=\infty$, $k_c=\frac{1}{8}$ and for $\beta=0$, $k_c=\frac{1}{4}$. It is known that the crossover region in the pure SU(3) gauge theory is around $\beta=5.3$ and beyond this point the string tension starts to follow the asymptotic-freedom prediction.^{6,25} From the string-tension data of Refs. 6 and 25 we get an estimate for the cutoff $a(\beta)$, using as input the Regge slope $\alpha'=0.90 \text{ GeV}^2$. This last quantity is related to the string tension T (in a relativistic string model) by $T=1/(2\pi\alpha')$. We shall use therefore $\sqrt{T}=420 \text{ MeV}$. Table I contains, for the values of β we have studied the values of the cutoffs and of the scale parameter Λ_0 of lattice QCD,

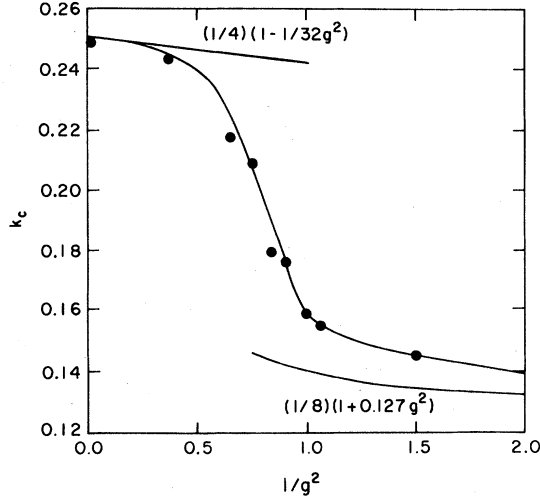


FIG. 1. Qualitative behavior of k_c as a function of $1/g_0^2$. The expected strong- and weak-coupling behavior is also shown.

$$\Lambda_0 = \frac{1}{a} (\gamma_0 g_0^2)^{-\gamma_1/2\gamma_0^2} \exp \left[\frac{1}{2\gamma_0 g_0^2} \right],$$

$$\gamma_0 = \frac{11}{3} (N/16\pi^2),$$

$$\gamma_1 = \frac{34}{3} (N/16\pi^2)^2$$
(3.1)

(with $N=3$), and the corresponding values of Λ_{MOM} (MOM refers to the momentum-subtraction scheme) obtained by replacing g_0 by $g_{0\text{MOM}}$ (Ref. 26),

$$\frac{6}{g_{0\text{MOM}}^2} = \frac{6}{g_0^2} - 2.741,$$
(3.2)

and multiplying the Λ_0 by π . We decide that Λ_0 and \sqrt{T} are related by $\Lambda_0 \simeq 0.0078 \sqrt{T}$ (Ref. 25) (which corresponds to $\Lambda_{\text{MOM}} \simeq 205$ MeV and $\Lambda_{\text{MS}} \simeq 70$ MeV, where MS refers to the minimal-subtraction scheme). The table contains also the corresponding anomalous dimensions $(3\alpha_B)^{-4/11}$, with $\alpha_B = 3/2\pi(\beta - 2.741)$, that will be used to compute renormalization-group-invariant quantities.²⁷

Our results for the masses are reported in Tables II–IV and are shown in Figs. 2 ($\beta=5.6$), 3 and 4

($\beta=6.0$), and 5 ($\beta=6.4$). The details on how the masses are extracted from the correlation functions and the error estimates will be discussed in the following paragraphs. At $\beta=5.6$ we have good control over the light-meson and baryon masses. Let us tentatively try to fit all the masses by linear plus quadratic functions of m . This is of course not the only way to analyze the data. We will later reanalyze the same data at all three values of β in a different way, that will not rely on any fitting procedure, in part to check the consistency of our results. We estimate $k_c \simeq 0.175$ and for small m we can fit the data by

$$\begin{aligned} m_P^2 &= 4.3ma^{-1} + O(m^2), \\ m_V^2 &= 0.70a^{-2} + 3.0ma^{-1} + \dots, \\ m_S^2 &= 1.10a^{-2} + 3.3ma^{-1} + \dots, \\ m_A^2 &= 1.6a^{-2} + 2.9ma^{-1} + \dots, \\ m_T^2 &= 1.7a^{-2} + 2.8ma^{-1} + \dots, \\ m_{P'}^2 - m_P^2 &= 2.0a^{-2} + O(ma^{-1}), \\ m_{V'}^2 - m_V^2 &= 2.5a^{-2} + \dots, \\ m_N &= 1.0a^{-1} + 5m + O(m^2a), \\ m_\Delta &= 1.35a^{-1} + 3.9m + \dots \end{aligned}$$
(3.3)

and at this value of β $a^{-1} \simeq 915$ MeV (from the string-tension data or from the ρ - π splitting). The statistical error in the data for the masses is of order ten percent (slightly better for the P, V states and slightly worse for the S, A, T and baryon states). Also, finite-size effects seem in our case in general to lead to an overestimate of the mass. Especially for the nucleon and Δ there are in addition systematic errors due to the small box size at this value of β (see the discussion below). For the radial excitations the error is around 30%.

At $\beta=6.0$ the masses seem to scale in agreement with the predictions of the renormalization group: they become smaller in lattice units. We find $k_c \simeq 0.158$ and a fit to our data with increased statistics (for details see Table III) is given by

TABLE I. The QCD scale parameter in lattice units, the inverse lattice spacing (the high-momentum cutoff being π/a), an anomalous-dimension factor, the size of the box in the space direction in fm, and the inverse size in the time direction (the effective temperature in MeV), as a function of $\beta=6/g_0^2$.

β	Λ_0	Λ_{MOM}	a^{-1}	$(3\alpha_B)^{4/11}$	$L_s = 5a$	$L_t^{-1} = (8a)^{-1}$
5.6	0.00362	0.231	915	0.78	1.1	110
6.0	0.00235	0.151	1380	0.74	0.73	170
6.4	0.00149	0.098	2050	0.71	0.49	260

TABLE II. Masses (in lattice units) of the pseudoscalar, vector, scalar, and axial-vector mesons and spin- $\frac{1}{2}$ and spin- $\frac{3}{2}$ baryons as a function of k at $\beta=5.6$. The second column lists the number of configurations used.

k	Conf.	m_P	m_V	m_S	m_A	m_N	m_Δ
0.120	3	2.30	2.31	2.85	3.00	3.81	3.82
0.130	6	1.96	1.98	2.19	2.22	3.43	3.44
0.135	3	1.84	1.86	1.95	1.83	3.13	3.14
0.140	6	1.70	1.74	1.80	1.75	2.90	2.93
0.145	3	1.58	1.62	2.05	1.98	2.95	2.99
0.150	16	1.37	1.44	1.82	1.71	2.44	2.50
0.155	13	1.31	1.42	1.88	1.91	2.32	2.35
0.160	36	1.08	1.27	1.43	1.53	1.91	2.01
0.165	36	0.82	1.08	1.32	1.34	1.71	1.86
0.170	3	0.72	1.01	1.1	1.4	1.4	1.7

$$\begin{aligned}
m_P^2 &= 3.1ma^{-1} + 3.6m^2 + O(m^3), \\
m_V^2 &= 0.30a^{-2} + 2.3m + O(m^2), \\
m_S^2 &= 0.5a^{-2} + 2.3m + \dots, \\
m_A^2 &= 0.65a^{-2} + 2.3m + \dots, \\
m_T^2 &= 0.7a^{-2} + 2.3m + \dots, \\
m_{P'}^2 - m_P^2 &= 1.0a^{-2} + \dots, \\
m_{V'}^2 - m_V^2 &= 1.7a^{-2} + \dots, \\
m_N &= 0.7 + 3.5m + \dots, \\
m_\Delta &= 0.9 + 3m + \dots
\end{aligned} \tag{3.4}$$

with again a statistical error in the data points of order 10 to 20%, except for the radial excitations P' and V' for which the error is of order 30 to 40%. We note that because of the higher statistics we have now been able to separate more accurately than in Ref. 2 the different terms in the expansion in m . At this value of the coupling constant $a^{-1} \simeq 1380$ MeV and the box size is therefore $\simeq 1$ fm.

For $\beta=6.4$ the cutoff is rather high $a^{-1} \simeq 2050$ MeV and we expect to get reliable estimates for

heavier-quark systems. For k_c we find $\simeq 0.156$ and in the region of the charmed states ($\eta_c, J/\psi, \dots$) which corresponds to $m \simeq 0.43a^{-1}$ ($k \simeq 0.133$) we find

$$\begin{aligned}
m_V^2 - m_P^2 &= 0.17a^{-2}, \\
m_S^2 - m_P^2 &= 0.6a^{-2}, \\
m_A^2 - m_P^2 &= 0.8a^{-2}, \\
m_T^2 - m_P^2 &= 1.0a^{-2},
\end{aligned} \tag{3.5}$$

with a 10–20% error on the mass difference, except for the last mass difference for which the error is more around 30%.

When we multiply the dimensionless masses by the appropriate power of the lattice spacing we obtain formulas that express the physical hadron masses in terms of m . This quantity is not a renormalization-group invariant but

$$m_R = (3\alpha_B)^{-4/11} m \tag{3.6}$$

is,²⁷ and we shall use this quantity instead. To take data at different values of β is crucial in order to test if we are in the scaling region where the hadron

TABLE III. Same as in Table II, but at $\beta=6.0$.

k	Conf.	m_P	m_V	m_S	m_A	m_N	m_Δ
0.100	3	2.64	2.64	2.65	2.65	4.20	4.20
0.120	6	1.97	2.02	2.02	2.08	3.19	3.20
0.125	3	1.69	1.70	1.82	1.87	2.60	2.61
0.130	16	1.63	1.65	1.81	1.83	2.59	2.61
0.135	16	1.48	1.52	1.59	1.62	2.21	2.23
0.140	26	1.13	1.18	1.38	1.43	1.72	1.76
0.145	26	1.01	1.08	1.18	1.31	1.57	1.65
0.1475	26	0.89	0.97	1.13	1.23	1.35	1.46
0.150	31	0.75	0.90	0.96	1.10	1.32	1.44
0.1525	12	0.68	0.80	0.82	0.96		

TABLE IV. Same as in Table II, but at $\beta = 6.4$.

k	Conf.	m_P	m_V	m_S	m_A	M_N	m_Δ
0.130	23	1.60	1.62	1.86	1.90	2.70	2.71
0.135	27	1.39	1.45	1.66	1.78	2.23	2.26
0.140	27	1.24	1.33	1.37	1.50	2.0	2.05
0.145	13	0.92	1.03	1.04	1.04	1.5	1.6
0.150	13	0.6	0.7				

masses (if measured in GeV at a fixed value of renormalization-group-invariant mass m_R or of the pseudoscalar mass) are β -independent.

Now in order to transform the data (Tables II–IV) we have obtained into hadron masses in MeV we have to analyze them. Of course the final result will depend on the prejudices of the analyzer; in certain cases we will be able to give a definite prediction for the masses, in other cases we will show the compatibility of our results with the experimental situation in the real world.

As usual our data are affected by two sources of error: statistical and systematic. The masses on the graphs are computed using the average value of the correlation function of the operator with the same quantum numbers as the particle. For the baryons we used their SU(6) wave functions in the time direction. The masses are estimated by fitting the correlation functions at the largest value of the time

$t=L_t/2$ to $A \cosh(L/2-t)m$ for mesons and $A \exp(-tm)$ for baryons. The difference between baryons and mesons is due to the fact that in the fermionic propagator at zero spatial momentum in the higher components positive-parity states propagate in the positive time direction and negative-parity states propagate backwards. The baryon propagator should be fitted to

$$A_+ \exp(-tm_+) + A_- \exp[-(L_t-t)m_-] \quad (3.7)$$

We see clearly from our data that $m_- > m_+$ and therefore the contribution proportional to A_- can be neglected at $t=L/2$ (we have not attempted to give a precise estimate of $m_- - m_+$). In producing the fits we have tried to include the effects of the excited states. This gives rise to a small downward ($\sim 5\%$) shift in the meson masses, but overall already the simple one-hyperbolic-cosine fit gives reasonable results, which is not unexpected since experimentally it is known that the radial excitations are high in mass for the mesons. On the other hand a two-mass fit is mandatory for the baryons, for which the simple exponential fit tends to overestimate the masses by as much as 20–30%. Again

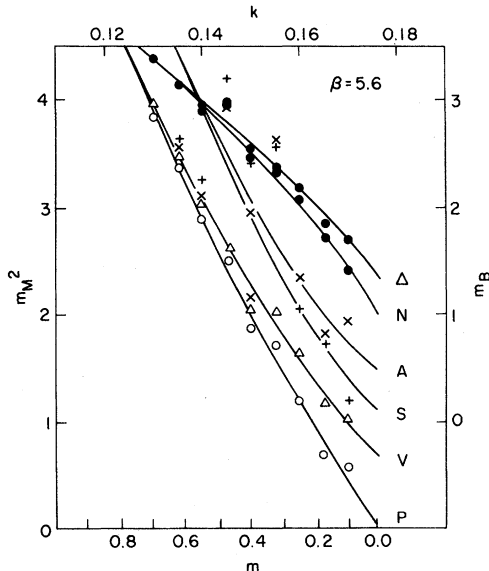


FIG. 2. Meson masses squared and baryon masses (in lattice units) as a function of k and the quark mass m [defined in Eq. (2.2)] at $\beta = 5.6$. P (0), V (Δ), S (+), and A (\times) label pseudoscalar ($J^{PC}=0^{-+}$), vector (1^{-}), scalar (0^{++}), and axial-vector (1^{++}) states. N and Δ (\bullet) label the nucleon ($\frac{1}{2}^{+}$) and Δ ($\frac{3}{2}^{+}$) states.

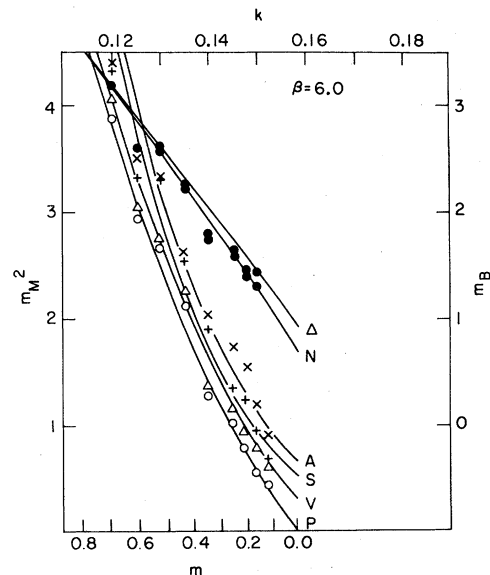


FIG. 3. Same as in Fig. 2 but at $\beta = 6.0$.

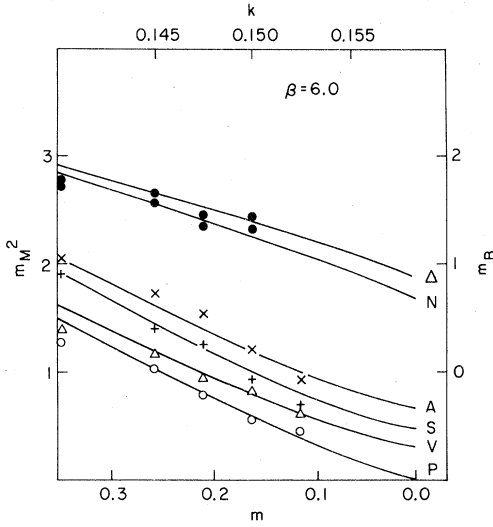


FIG. 4. An enlarged view of the small-mass region at $\beta = 6.0$. Notation as in Fig. 2.

this is not expected since the mass difference among radial recurrences is smaller for the baryons than for the mesons. This is the first source of our systematic errors. The second one comes from finite lattice effects in the spatial direction. For large lattices of space dimension L we have a shift (δE) in the energy of a particle at rest which is equal to

$$6V_p^{(L)} \propto 6C \exp(-m_\pi L)/L, \quad (3.8)$$

where V is the Yukawa potential between two P particles at rest and is a function of the distance. Equation (3.8) can easily be obtained from the theory of images. Since the constant C is in general not ex-

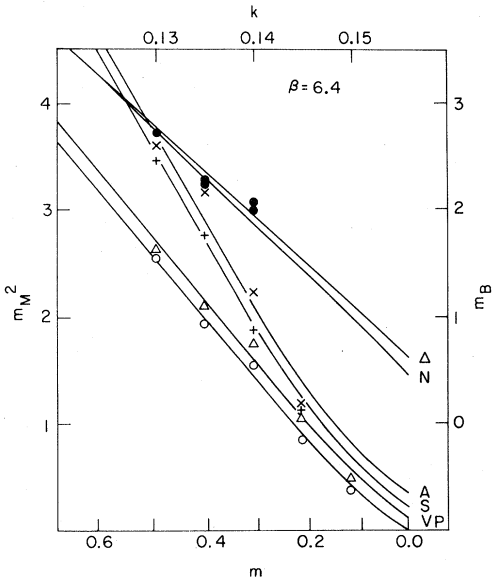


FIG. 5. Same as in Fig. 2 but at $\beta = 6.4$.

pected to be small, one should always try to keep $m_\pi L$ large. We should remember also that the system is at a temperature $T = 1/aL$. If T becomes greater than the transition between confined and unconfined vacuum, the long-range tail of the quark potential is seriously modified and the masses of the light states may get drastically changed.

A different source of error which is present in the Wilson formulation, but not in the Kogut-Susskind formulation for the fermion, is due to the fact that, mathematically speaking, the average value of quantities like the meson propagator is strictly infinity for any $k > \frac{1}{8}$ and for a finite volume. We have considered lattices where the bosonic degrees of freedom N are of order 10^5 . The energy density is not fixed and there are oscillations of order $N^{-1/2}$. This means that the probability of having a configuration of zero energy (pure gauge) is of order $\exp(-N)$, which is clearly very small but not zero. Since for a pure gauge configuration (free case) the Green's functions are infinite for $k > \frac{1}{8}$, one expects to find divergent results in this range. In practice this happens only if the number of gauge configurations sampled is of order $\exp(10^5)$ for our lattices, which is not definitely our case. However let us consider what happens at values of k larger than $\frac{1}{8}$. In a rough approximation $k_c - \frac{1}{8}$ is proportional to E and one expects fluctuations in k_c from configuration to configuration with a Gaussian distribution and a width proportional to $N^{-1/2}$:

$$P(K) \exp[-A(k - k_c)^2 / Nk_c^2]. \quad (3.9)$$

This means that we must stay in the region where

$$N_c \ll \exp[A(k - k_c)^2 / Nk_c^2], \quad (3.10)$$

N_c being the number of gauge configurations one is considering.

Unfortunately the fluctuations in the value of k_c are larger than what one would expect from a pure energy argument (we estimate $A \sim 10^4$). This can be seen by large memory effects. In performing the Monte Carlo iterations the correlation from the energy after N steps and after $N + M$ steps is practically negligible after $M \simeq 10$. On the other hand there is a strong correlation at this value of M , and in order to have independent measurements of the Green's functions and minimize the statistical errors we have considered sets of configurations separated by 100 Monte Carlo steps (with ten hits per site) (some correlation among configurations is unfortunately still present). We hope to have in part reduced these effects by using completely statistically independent starting configurations, thermalized with $\sim 3 \times 10^3$ Monte Carlo steps. It is conceivable that these effects are due to hopping between config-

urations with different topological number (which is a slow process), but we do not know how to substantiate this suggestion. In our previous work (Ref. 2) we were not aware of this strong correlation and we were not careful in intercalating many unused gauge configurations between the ones we used, and this caused an underestimate of our statistical errors and a general overestimate of the masses in lattice units at $\beta=6.0$. (This effect may also be one of the reasons for the discrepancy of our results with those of Ref. 28.)

Of course all these systematic effects vanish when k goes away from k_c and we have taken most of our data in what we believe to be a safe region. In particular we have chosen not to take any more data at $\beta=6.0$, $k=0.155$ because of possible finite-size effects and the closeness of k_c .

After having obtained the true mass at a given value of β and k , one still must extrapolate to $\beta \rightarrow \infty$, and this can be done using the renormalization group. We notice however that after we have adjusted the value of k to have a preassigned ratio for the masses of two particles (e.g., π/ρ), the masses of all the other particles, (e.g., in units of the ρ mass) must show a systematic dependence on β which vanishes like $\exp(-c\beta)$ for large β . This is in contrast with ratios like $m_\rho/\Lambda_{\text{MOM}}$ which have corrections proportional to inverse powers of β . The size of these effects can be partially estimated by doing computations at different values of β (unfortunately also the other systematic effects are strongly β -dependent).

Let us go back to the statistical errors. Their direct estimate is not a simple matter. The most straightforward procedure is to compare mass estimates obtained by averaging the correlation functions over different sets of, say, ten configurations, each separated by 100 to 200 Monte Carlo steps, and where by different we mean obtained from different starting configurations. One should keep in mind that the process of averaging the correlation functions and then computing the masses is not the same as averaging masses.

As far as we have used different configurations for different values of k , and since we believe that the masses are smooth functions of k , the oscillations of the estimated masses when we vary k is a good estimate of the error, as long as the configurations are independent of each other. The use of correlated configurations was, as we explained, the reason for the underestimate of the errors in Ref. 2. A careful study of the statistical errors at $\beta=6.0$ (using a total of 32 gauge configurations at $k=0.130, 0.145, 0.1457, 0.150$, and 0.1525 on lattices $5^3 \times 10$ and with up to 100 relaxation iterations) will be reported in Ref. 29.

Let us now turn to a discussion of the pion mass. We will assume that m_π^2 vanishes linearly at k_c like $k - k_c$. This is certainly reasonable from our data at $\beta=5.6$. The fits give, for small m ,

$$\begin{aligned} m_P^2 &= 4.2m, \quad k_c = 0.175, \quad \beta = 5.6, \\ m_P^2 &= 3.1, \quad k_c = 0.158, \quad \beta = 6.0. \end{aligned} \quad (3.11)$$

The error in k_c may be roughly estimated at 10^{-3} and that on the slope should be around 10–20%. Now if we introduce the renormalization-group-invariant mass $m_R = (3\alpha_B)^{-4/11}m$ we get

$$m_P^2 = S(\beta)m_R \quad (3.12)$$

with

$$S(5.6) = 3.3, \quad S(6.0) = 2.3. \quad (3.13)$$

Since S has dimensions of a mass, $S(\beta)/\Lambda_{\text{MOM}}(\beta)$ should be a constant. Using Table I we find

$$\begin{aligned} S(5.6)/\Lambda_{\text{MOM}}(5.6) &= 14, \\ S(6.0)/\Lambda_{\text{MOM}}(6.0) &= 15 \end{aligned} \quad (3.14)$$

which is constant inside the errors. Using the value $\Lambda_{\text{MOM}} = 210$ MeV we get the estimate

$$m_P^2 \simeq (1600 \text{ MeV})(m_R^a + m_R^b). \quad (3.15)$$

Where we have replaced $m_R \rightarrow (m_R^a + m_R^b)/2$ and a and b label the quark flavor. This implies for the average value of the renormalization-invariant up and down quark masses, using the pion mass as input,

$$(m_u + m_d)/2 \simeq 6 \text{ MeV}. \quad (3.16)$$

Using the kaon mass ($m_K = 495$ MeV) as input we find from the graph at $\beta=5.6$ or the above formula

$$(m_d + m_s)/2 \simeq 77 \text{ MeV} \quad (3.17)$$

Using alternatively the current-algebra relations $m_d/m_u = 1.8$ and $m_s/m_d = 2.01$ (Ref. 30) we find

$$\begin{aligned} m_u &\simeq 4.5 \text{ MeV}, \quad m_d \simeq 8 \text{ MeV}, \\ m_s &\simeq 160 \text{ MeV} \end{aligned} \quad (3.18)$$

in agreement with phenomenological estimates. The goodness of the scaling between $\beta=5.6$ and $\beta=6.0$ can be seen by plotting m_P (Fig. 6) or m_P^2 (Fig. 7) versus m_R on the same graph and using physical units (MeV). The points should lie on the same universal curve. This happens inside the errors in our data, especially in the region of small masses. We see that for small masses m_P is proportional to $m_R^{1/2}$ and changes to a linear dependence at higher masses.

We are able to consider explicitly the case of strange particles, and the masses of the lighter states

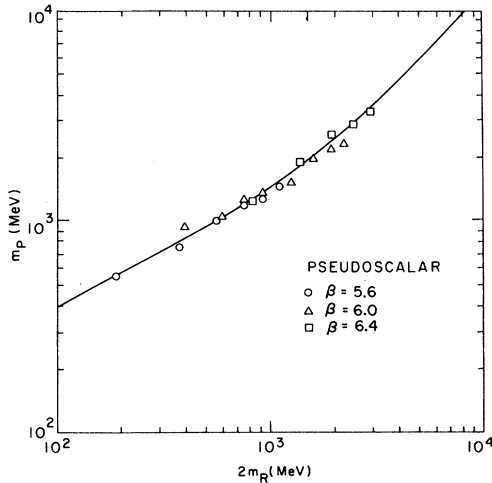


FIG. 6. Pseudoscalar-meson mass in physical units as a function of the renormalized mass. The data at $\beta=5.6$, 6.0, and 6.4 have been combined together. The line is only intended as a guide to the eye.

are obtained by extrapolation. Deviations from linearity in the mass squared of the pseudoscalar particles going from the strange to the up and down quarks is proportional to the violations of the Gell-Mann—Okubo sum rules, which are known to be small.

The points we have at $\beta=6.4$ are for masses that are not small enough to see $m_P^2 \propto m$, and our estimate for k_c is more shaky. We can fix k_c by requiring that $S(\beta)$ continues to scale with β , and find

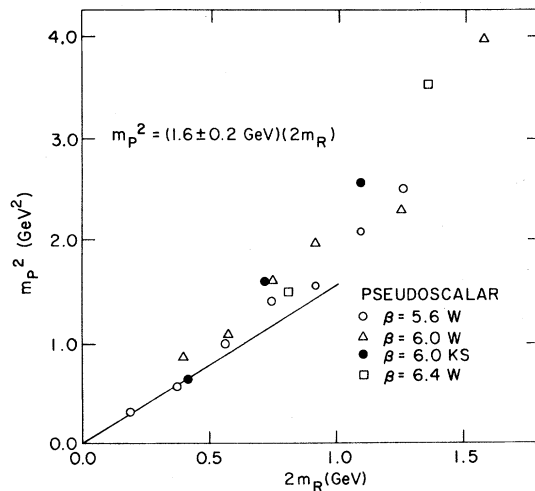


FIG. 7. The behavior of the pseudoscalar-meson mass for small quark mass. Data for different values of β and different actions (W=Wilson action, KS=Kogut-Susskind action) have been combined. The line is only intended as a guide to the eye.

$k_c \simeq 0.156/0.157$. At this value of β the mass gap (the glueball mass) is $\simeq 1300/2050 \simeq 0.6$ in lattice units, and this should allow us to still get reasonable estimates for the charm states. We hope (but of course it would be useful if the results could be checked on larger lattices) that since the J/ψ spectroscopy is sensible to the quark potential at moderate distances the final results are not affected by the relatively small box size. Our estimates for the masses of some of the $c\bar{c}$ states are shown in Table V. For the mass of the charmed quark we find

$$m_c \simeq 1300 \pm 100 \text{ MeV} \quad (3.19)$$

which is slightly lower than potential-model estimates.³¹

Let us now study the ρ mass. A first possibility would be to do the same plot of m_V versus k as in the case pseudoscalar. In this case a linear (or linear + quadratic) fit in a wide k range is rather good (see Figs. 8 and 9), giving for the extrapolated value at k_c 0.84 at $\beta=5.6$ and 0.55 at $\beta=6.0$, with an error of about 10%. Translated in MeV this gives a mass about 750 MeV.

The situation is not so nice however if we consider data at k not too close to k_c . To see it clearly we can study the dependence of $m_V^2 - m_P^2$ or m_P^2 . This number is in the physical case practically constant when one goes from the ρ to the J/ψ . The data are shown in Fig. 10. One can clearly see that it does not scale for large mass and is compatible with an extrapolation at zero mass of about 0.6 GeV.² Only for larger β ($\beta=6.4$) there is a signal of approximately mass-independent splitting. The fact that the spin splittings do not come right until the pseudoscalar mass becomes of order one or less in lattice units should not come entirely as a surprise. Spin effects in the masses using the Wilson action are strongly suppressed if one is not near enough to the continuum limit. This means that we have to go to masses of the quarks of order 0.2/0.3 in lattice units in order to see in a decent way the spin-spin effects. Analogous plots for the other mesons are shown in Figs. 11–14.

Spin forces are also responsible for the splitting

TABLE V. Masses of $c\bar{c}$ mesons, in MeV. Experimental numbers in parentheses.

J^{PC}	$c\bar{c}$	
0^{-+}	$\eta_c(2980)$	3000 ± 30
1^{--}	$J/\psi(3097)$	
0^{++}	$\chi_0(3414)$	3400 ± 50
1^{++}	$P_c(3507)$	3500 ± 50
1^{+-}		3600 ± 100

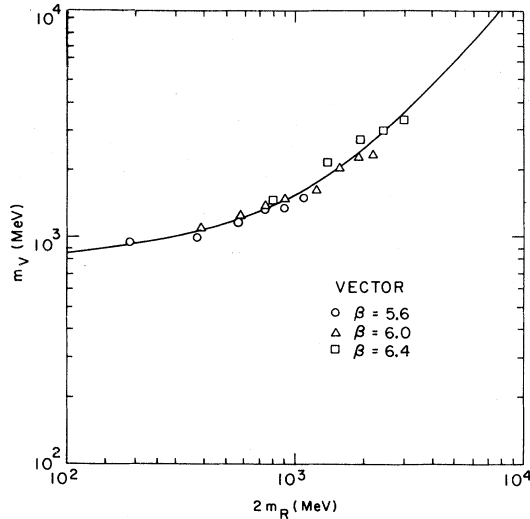
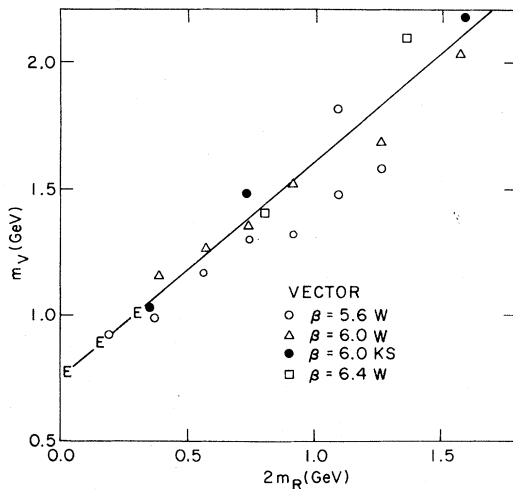
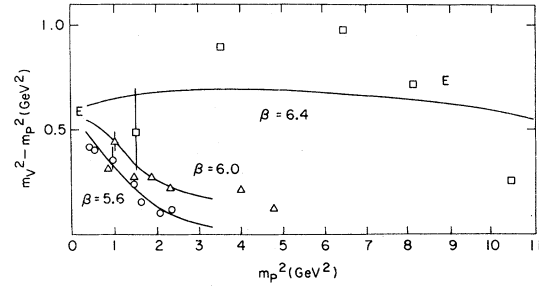


FIG. 8. Same as Fig. 6 but for the vector.

between the $J = \frac{1}{2}$ (Figs. 15 and 16) and $J = \frac{3}{2}$ (Figs. 17 and 18) baryons. Since again the spin-spin effects vanish when the masses are large, it is better for baryons to consider the difference in mass squared versus the pseudoscalar meson mass (with of course the same average quark mass in both cases). In Fig. 19 we show $m_{3/2}^2 - m_{1/2}^2$ versus m_p^2 . The data are fluctuating so that it is not clear how to perform an extrapolation to $k = k_c$ or $m_p^2 = 0$ (it will depend on the functional form assumed). Our data seem to indicate a value between 0.6 and 0.7 GeV^2 , but we prefer to show for comparison the experimental points. (We have used the mass of the p and Δ for the light-quark case.) In or-

FIG. 9. Same as Fig. 7 but for the vector. E are the experimental masses for ρ , K^* , and ϕ .FIG. 10. Mass squared difference, in physical units, for the vector and pseudoscalar mesons, as a function of the pseudoscalar mass squared. The lines are only intended as a guide to the eye. E are the experimental values for ρ - π and J/ψ - η_c .

der to know the mass of a state containing three strange quarks, we have used Ξ and Λ for the octet and estimated the mass of such an object to first order in SU(3) breaking giving a mass of about 1495 MeV for the octet. The experimental data are clearly compatible with the theoretical ones.

In our search for a quantity stable as a function of m_p^2 we have computed the ratios $(m_{3/2}^2 - m_{1/2}^2)/(m_V^2 - m_S^2)$. The spin splittings are small for both mass differences, but their ratio seems to be remarkably constant (within our large error bars). We show this quantity in Fig. 20. Our data seem to indicate

$$(m_{3/2}^2 - m_{1/2}^2)/(m_V^2 - m_S^2) \simeq 1.1 \pm 0.3 \quad (3.20)$$

to be compared with the experimental value of 1.11 for the Δ - N - ρ - π case.

Let us finally consider the splittings between the $L = 1$ and $L = 0$ multiplets. We do not have enough

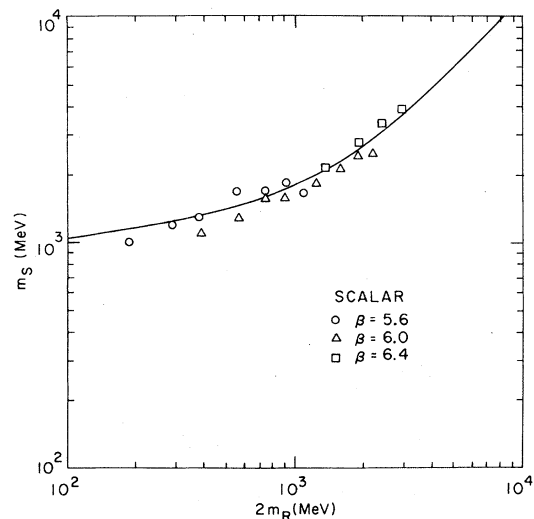


FIG. 11. Same as Fig. 6 but for the scalar meson.

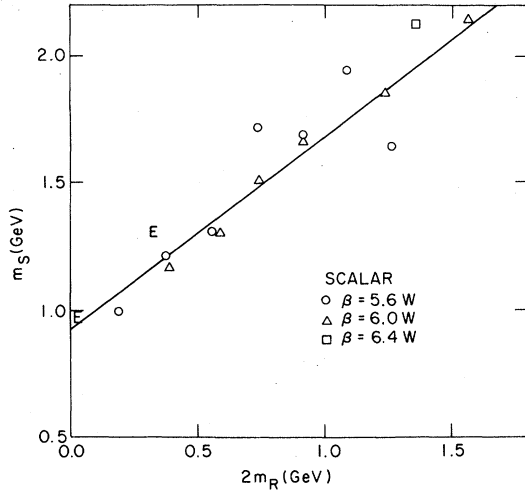


FIG. 12. Same as Fig. 7 but for the scalar meson. E are the experimental values for δ and ϵ .

statistics to estimate the splitting between the δ and A_1 in a clear way, although we see that the A_1 is heavier than the δ . If we extrapolate the masses of the scalar and axial vector at $m_p^2=0$ (see Figs. 12 and 14) we obtain

$$m_\delta = 950 \pm 150 \text{ MeV} \quad (3.21)$$

and

$$m_{A_1} = 1100 \pm 150 \text{ MeV} . \quad (3.22)$$

As a consequence of using the Wilson action the spin splittings in the $L=1$ multiplet die off rather quickly when the mass increases.

The ratio $(m_A^2 - m_S^2)/(m_V^2 - m_P^2)$ seems again

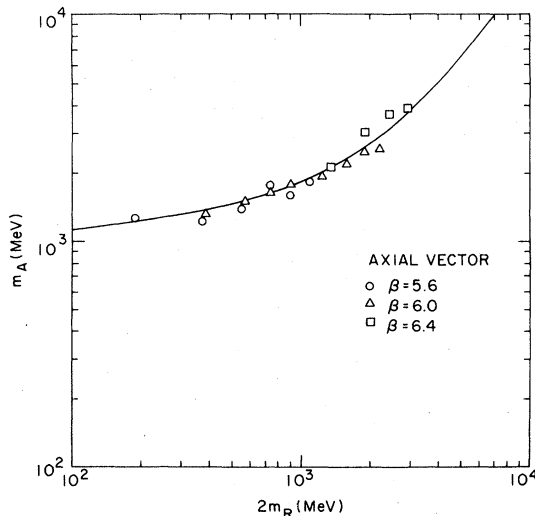


FIG. 13. Same as Fig. 6 but for the axial-vector meson.

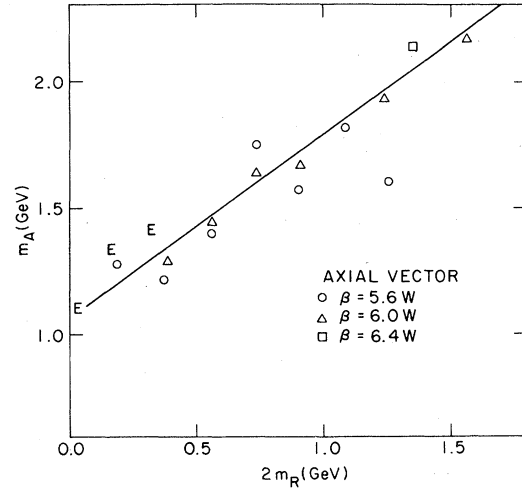


FIG. 14. Same as Fig. 7 but for the axial vector. E are the experimental numbers of the A_1 , Q_A , and E.

more or less independent of m_p^2 and we find a value of 0.7 ± 0.3 , using again our data at all three values of β . Still one should keep in mind that by elementary considerations the radius of the $L=1$ states is expected to be larger than the $L=0$ states, and decreasing the size of the box from 1.1 to 0.5 fm in going from $\beta=5.6$ to $\beta=6.4$ may affect the mass splittings. However we do not have a simple way to estimate this effect.

We have also looked at the mass of the 1^{+-} (tensor) state. With our errors we cannot clearly see it split from the axial vector. All we can say in general is that in the small-mass limit it seems to be higher in mass, by an amount that is comparable to or less than our errors (~ 100 MeV).

From the subdominant corrections to the pseudo-

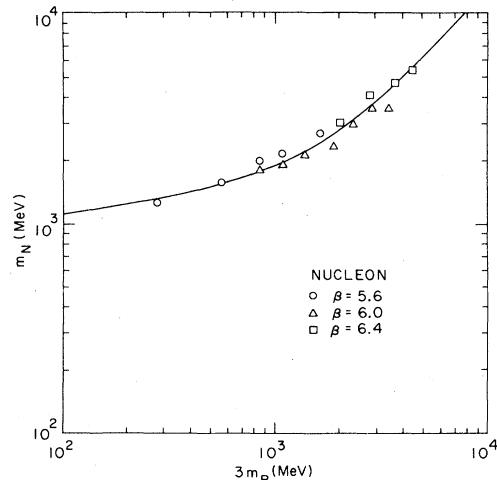


FIG. 15. Same as Fig. 6 but for the nucleon.

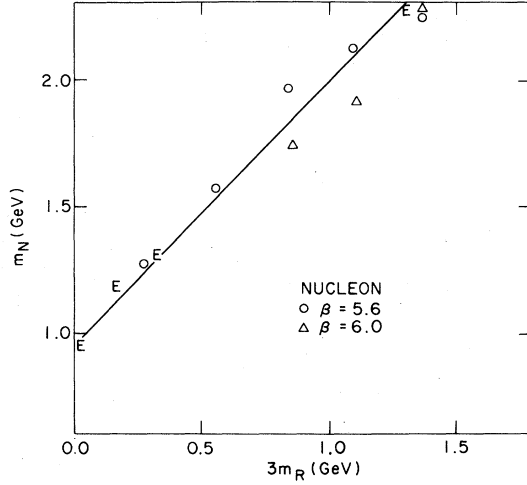


FIG. 16. Same as Fig. 7 but for the nucleon. E are the experimental points for N , Σ , Ξ , and Λ_c .

scalar and vector propagator we have tried to estimate the mass of the first radially excited states. We find values in the 1.2–1.9 GeV range in qualitative agreement with experiment, but some care must be used because the masses are relatively high with respect to the inverse lattice spacing.

IV. THE $r=0$ CASE

In this section we will study what happens when we use the fermions with $r=0$. We mentioned before that it is possible in this case to diagonalize the fermion propagator and reduce the number of fermion flavors from 16 to 4. The existence of 4 fermion species does not give rise to any problem as far as the mesons are concerned. However it gives us serious problems (which we have not been able to

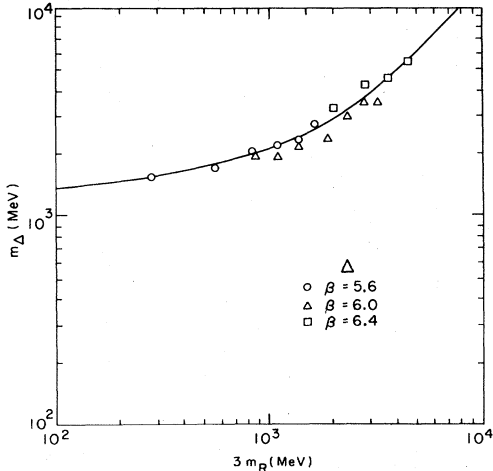


FIG. 17. Same as Fig. 6 but for the Δ .

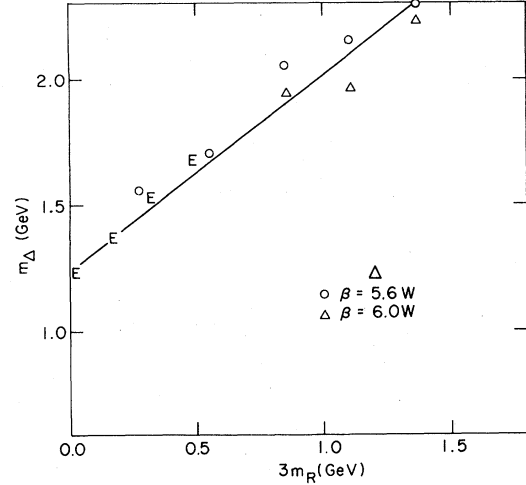


FIG. 18. Same as Fig. 7 but for the Δ . E are the experimental points for Δ , Σ^* , Ξ^* , and Ω .

solve) in the baryon sector, especially with respect to the distinction of baryons with $I=\frac{1}{2}$ and $I=\frac{3}{2}$.

The main quantities that we study are the meson propagator

$$M_M(\vec{n}) = \sum_{ab} |G_q^{ab}(\vec{n})|^2 \quad (4.1)$$

and the baryon propagator

$$M_B(\vec{n}) = \sum_{abc} \sum_{a'b'c'} \epsilon^{abc} \epsilon^{a'b'c'} G_q^{aa'}(\vec{n}) G_q^{bb'}(\vec{n}) G_q^{cc'}(\vec{n}). \quad (4.2)$$

Let us first discuss the meson case. Particles with different spin-parities sit at different corners of the Brillouin zone for the propagator $M_M(\vec{n})$. It is therefore convenient to set the external momentum equal to zero (mod π) and consider the four kinds of corners of the spatial Brillouin zone. We define, following the suggestion of Ref. 20,

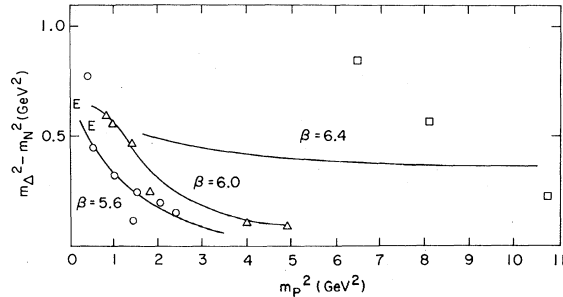


FIG. 19. Mass difference squared, in physical units, for the Δ and nucleon, as a function of the square of the pseudoscalar mass. The lines are only intended as a guide to the eye. E are the experimental points for Δ/N and Ω .

$$\begin{aligned}
M_M^0(n_t) &= \sum_{n_x, n_y, n_z} M_M(\vec{n}), \\
M_M^1(n_t) &= \sum_{n_x, n_y, n_z} [(-1)^{n_x} + (-1)^{n_y} + (-1)^{n_z}] M_M(\vec{n}), \\
M_M^2(n_t) &= \sum_{n_x, n_y, n_z} [(-1)^{n_x+n_y} + (-1)^{n_y+n_z} + (-1)^{n_z+n_x}] M_M(\vec{n}), \\
M_M^3(n_t) &= \sum_{n_x, n_y, n_z} (-1)^{n_x+n_y+n_z} M_M(\vec{n}).
\end{aligned} \tag{4.3}$$

If we go back to the original action (before diagonalization) it is easy to see that for large n_t we have

$$\begin{aligned}
M_M^0(n_t) &\simeq \exp(-m_P n_t), \\
M_M^1(n_t) &\simeq \exp(m_V n_t) + (-1)^{n_t} \exp(-m_T n_t), \\
M_M^2(n_t) &\simeq \exp(-m_V n_t) + (-1)^{n_t} \exp(-m_A n_t), \\
M_M^3(n_t) &\simeq \exp(-m_P n_t) + (-1)^{n_t} \exp(-m_S n_t),
\end{aligned} \tag{4.4}$$

where m_P , m_V , m_S , m_A , and m_T are the masses of the lightest particles with the quantum numbers of π , ρ , δ , A , and B .

The analysis in the case of the staggered fermions, as we see, is more complicated because each propagator contains more than one particle. To measure the masses we have collected the data by generating altogether eight gauge-field configurations (compared to four in Ref. 2) on a 6^4 lattice at $\beta=6.0$, separated by 100 Monte Carlo iterations (with ten hits per link). The quark propagators have been computed for $m_R=0.3, 0.2$, and 0.1 on a $6^3 \times 12$ lattice, where the gauge-field configuration in the time direction has been doubled. The mass of the pion has been measured by fitting the pion propagator M_M^0 to a form

$$\begin{aligned}
M_M^0(n_t) &= A [\exp(-n_t m_\pi) + \exp(-12+n_t) m_\pi] \\
&\quad + B [\exp(-n_t) \\
&\quad \quad + \exp(-12+n_t) m_\pi].
\end{aligned} \tag{4.5}$$

The value of A is connected to $\langle 0 | \bar{\psi} \gamma_5 \psi | \pi \rangle$, and,

$$R_1(n_t) = \frac{\exp(-m_V n_t) + (-1)^{n_t} \exp(-m_T n_t) + (n_t \leftrightarrow 12-n)}{\exp(-m_P n_t) + (n_t \leftrightarrow 12-n)}. \tag{4.7}$$

In this way we obtain the results shown in Table VI and in Fig. 21. The error in the vector mass can be estimated (in the same way as the pseudoscalar) to a few percent (and neglecting of course the systematic errors coming from our biased procedure) and for the other masses to at least ten percent.

For the baryons we do not see any striking differ-

via the equations of motion

$$\partial_\mu A_\mu = m_q \bar{\psi} \gamma_5 \psi, \tag{4.6}$$

to f_π . The fit is rather good and the error on m_π coming from the fit can be estimated at a few percent.

The statistical error is harder to estimate. The two mass fits cannot be done on a single configuration. The simplest, but not the most rigorous, estimate can be obtained by considering as approximate mass (to be corrected later)

$$\frac{1}{2} \operatorname{arccosh} \left[\frac{G(4) + G(8)}{2G(6)} \right].$$

The masses do not seem to be too strongly correlated and the statistical error estimated with the standard ruled should be again of a few percent. Although larger runs seem to be needed in order to decide whether the configurations in the sample can be considered really statistically independent, the fluctuations in m_π could be smaller than in the $r=1$ case. This circumstance would lead us to confirm the hypothesis that the oscillations in the latter case are due to fluctuations in k_c (i.e., mass renormalization), whereas in the $r=0$ case $k_c = \infty$ for all β as a consequence of the γ_5 invariance. The error in m_π and f_π is of course larger.

When we estimate the other masses it is not possible, due to the smallness in the time direction of our lattice, to consider radial excitations. The simplest method that we have devised is to consider the ratio $R(n_t) = M^1(n_t)/M^0(n_t)$ and fit it to

ence between different corners of the Brillouin zone (and we are puzzled by the assignments). We therefore quote only the value of a common baryon mass. There the errors are somewhat larger, both statistical and systematic.

The baryon mass has been computed by studying the ratio of the baryon equivalent of M_M^0 to M_M^1 (for

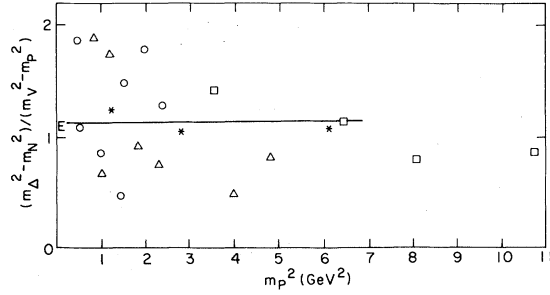


FIG. 20. Ratio of the difference in mass squared of the Δ and nucleon over the same quantity for the vector and pseudoscalar. The stars are the averages of the points at $\beta=5.6, 6.0,$ and 6.4 . E is the experimental ratio. The line is only intended as a guide to the eye.

the $J^P = \frac{3}{2}$). These results are also shown in Table VI. The last two lines in the table show the extrapolated results for the masses at $m_q=0$ in units of the lattice spacing and in MeV (assuming $a^{-1}=1500$ MeV, which is about 10% higher than the lattice spacing in the Wilson case).

Thus the mass spectrum for the mesons turns out to be rather satisfactory. On the other hand the mass of the baryon seems to be definitely too large. It is conceivable that we have not chosen the nucleon channel, and that our fitting procedure was too arbitrary. We leave this problem to a further theoretical investigation. However, especially in this case, as for the Wilson fermions, larger lattices would be helpful.

In conclusion it seems that the $r=0$ case gives rise to more stable and reliable estimates for the mesons (within our limited statistics), while difficulties are present for the baryons. The $r=1$ (Wilson) case presents no difficulties in the internal quantum-number assignments, and gives rise to correlation functions that do not have an oscillating part, but seems to suffer both from fluctuations in k_c and rather small spin-spin forces at not-too-small m . It would of course be interesting to see if an intermediate case, like $r = \frac{1}{2}$, shares some of the ad-

vantages of both methods. The choice of the best value of r is rather important and could be studied both empirically and in an analytic fashion in the framework of lattice perturbation theory. It is however interesting to note that the value of the ρ mass at $k=k_c$ seems to differ only by 10% at $\beta \simeq 6.0$, while at $\beta=0$ this difference was a factor of about 100%.

V. DECAY AMPLITUDES

From the long-distance falloff of the correlation function we can estimate, besides the mass of the state, also the amplitude of the wave function. For large time separations a meson propagator at zero lattice three-momenta will behave as

$$\tilde{M}_\Gamma(t,0) \underset{t \gg 1}{\sim} \frac{A_\Gamma}{2m_\Gamma} e^{-m_\Gamma t}, \quad (5.1)$$

where A_Γ is some numerical constant which is slowly varying in m_Γ . We have computed some of these constants as functions of the masses m_Γ at $\beta=5.6, 6.0,$ and 6.4 . In Table VII we display our results for the quantities $\gamma_\Gamma = 2k\sqrt{A_\Gamma}$ obtained using the Wilson fermion action. The factor $2k$ arises because of the connection between lattice and continuum fields in the Wilson formulation [see Eq. (2.4)]. The statistical errors in the γ 's is estimated at about 30%. In general an overestimate of the masses will lead to an overestimate of the amplitudes, so the errors in the two quantities are correlated. From the numbers in the table we can estimate the decay amplitudes. The couplings of the states to the currents are defined²⁷ as follows:

$$\begin{aligned} (m_1 + m_2) \langle 0 | \bar{\psi}_2 \gamma_5 \psi_1 | P \rangle &= \sqrt{2} f_P m_P^2, \\ (m_1 - m_2) \langle 0 | \bar{\psi}_2 \psi_1 | S \rangle &= f_S m_S^2, \\ \langle 0 | \bar{\psi}_2 \gamma_\mu \psi_1 | V \rangle &= f_V^{-1} m_V^2 e_\mu, \\ \langle 0 | \bar{\psi}_2 \gamma_5 \gamma_\mu \psi_1 | A \rangle &= f_A^{-1} m_A^2 e_\mu, \end{aligned} \quad (5.2)$$

where P, S, V, A label the different spin-parity states. For the pseudoscalar we find therefore f_P

TABLE VI. Quark mass; masses of pseudoscalar, vector, scalar, axial-vector, tensor, radial excitation of the pseudoscalar, baryon; and pseudoscalar decay constant at $\beta=6.0$ using the Kogut-Susskind fermion action on eight gauge-field configurations. All are in lattice units. In the fourth line the extrapolated values at $m=0$ are in lattice units, and in the last line in MeV, using $a^{-1}=1500$ MeV.

m	m_P	m_V	m_S	m_A	m_T	m_P	m_B	f_P
0.3	1.21	1.35	1.48	1.61	1.71	1.57	2.26	0.226
0.2	0.94	1.10	1.24	1.37	1.45	1.32	1.93	0.191
0.1	0.60	0.77	0.91	1.01	1.11	1.04	1.5	0.156
0.0	0	0.51	0.65	0.75	0.82	0.78	1.13	0.120
0.0	0	750	970	1120	1230	1170	1700	177

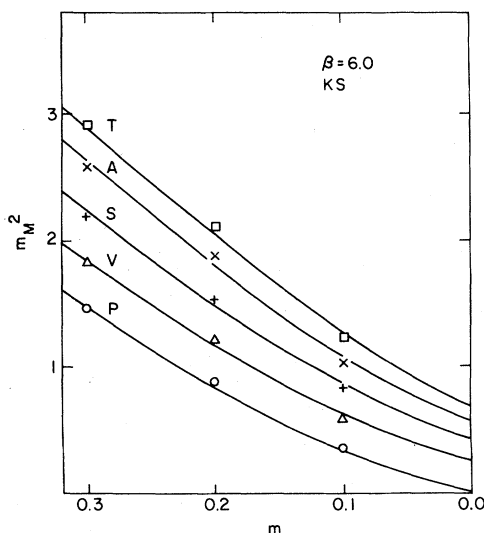


FIG. 21. Meson masses squared in lattice units as a function of the quark mass m at $\beta=6.0$ obtained using the Kogut-Susskind fermion action. The lines are only intended as a guide to the eye.

$=\sqrt{2}\gamma m/(m_p^2 a^2)$ and for the vector and axial-vector states we use $f_\Gamma^{-1}=\gamma(a^{-2}/m_\Gamma^2)$. The pseudoscalar decay constant is shown in Fig. 22 as a function of the pseudoscalar-meson mass squared. We can extrapolate our data to the small-quark-mass region and for the pion we find therefore

$$f_\pi = 150 \pm 50 \text{ MeV} \quad (5.4)$$

which is in not too good agreement with the experimental value 93.5 MeV.³² For the other states we

show some estimates in Table VIII. Again the agreement seems generally bad. In part this situation could be explained by one-loop corrections, which have not been taken into account. It is also quite possible that we have underestimated our systematic errors. From the decay amplitudes of the vectors one can then estimate their leptonic width,

$$\Gamma(V \rightarrow e^+ e^-) = \frac{1}{3} (\alpha e q)^2 m_V \left[\frac{4\pi}{f_V^2} \right]. \quad (5.4)$$

(The charge factor eq is already included in the number quoted in Table VIII.) Through the Van Royen-Weisskopf formula³³ f_V is related to the wave function of the $\bar{q}q$ pair at the origin

$$|\psi(0)|^2 = m_V^3 f_V^{-2} / 12. \quad (5.5)$$

Finally we should mention that we have attempted to compute the value of the proton wave function at the origin. This number is of interest for proton decay in grand unified theories. The evaluation of the amplitudes proceeds as in the meson case. At $\beta=6.0$ we find for the usually quoted parameter

$$\lambda = 0.051 \pm 0.02 \text{ GeV}^3. \quad (5.6)$$

Bearing on our experience with the meson case, we would expect this number to be above its true value, perhaps by again as much as a factor of 2, because of systematic effects due to not large enough β .

VI. THE MASS OF THE η'

In this section we will present some preliminary estimates for the mass of the η' . By setting the fer-

TABLE VII. Amplitudes $\gamma_\Gamma/\sqrt{12}$ for the pseudoscalar, vector, scalar, and axial-vector mesons as a function of β and k . The number of configurations used is the same as in Tables II-IV.

	k	P	V	S	A
$\beta=5.6$	0.150	0.36	0.29	0.21	0.17
	0.155	0.37	0.30	0.28	0.20
	0.160	0.30	0.27	0.10	0.14
	0.165	0.24	0.22	0.23	0.19
$\beta=6.0$	0.130	0.25	0.22	0.17	0.15
	0.135	0.24	0.22	0.15	0.13
	0.140	0.21	0.19	0.14	0.13
	0.145	0.20	0.16	0.13	0.10
	0.1475	0.16	0.15	0.14	0.10
	0.150	0.11	0.10	0.10	0.10
	0.1525	0.11	0.08	0.12	0.08
$\beta=6.4$	0.130	0.24	0.21	0.19	0.16
	0.135	0.24	0.21	0.19	0.20
	0.140	0.23	0.19	0.15	0.14

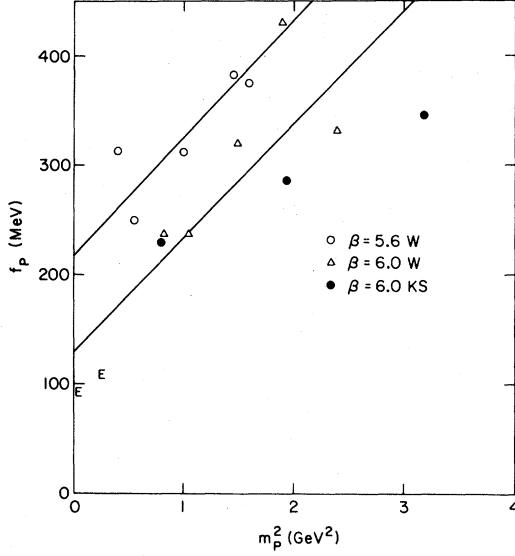


FIG. 22. The pseudoscalar decay constant (in MeV) as a function of the pseudoscalar mass. The lines are only intended as a guide to the eye. E are the experimental points for π and K mesons.

mionic determinant equal to a constant, we have excluded from the theory all effects that are due to dynamic-fermion loops. In particular we have excluded meson annihilation diagrams which are believed to be responsible for the nonconservation of the isoscalar axial-vector current and the large η' mass.¹⁵ In this section we will show how one can compute the effects on the meson masses of a class of annihilation diagrams, which are calculable in the no-loop approximation, that are leading to lowest order in the number of fermion flavors.

As an example to illustrate our strategy consider the free energy of a spin system in a field. For small field it is known in terms of zero-field correlation functions,

$$F(h) = F(0) + hF'(0) + \frac{1}{2}h^2F''(0) + O(h^3), \quad (6.1)$$

where

TABLE VIII. Decay constants (with appropriate charge factors included).

	This calculation	Experiment (Ref. 32)
f_ρ^{-1}	0.5 ± 0.1	0.19
f_ϕ^{-1}	0.2 ± 0.1	0.075
r_{A_1}	0.3 ± 0.1	0.11
$f_{J/\psi}^{-1}$	0.2 ± 0.1	0.083

$$F''(0) = M = \frac{1}{V} \left\langle \sum_x \phi_x \right\rangle, \quad (6.2)$$

$$F'''(0) = \chi = \frac{1}{V} \left[\left\langle \sum_{x,y} \phi_x \phi_y \right\rangle - \left\langle \sum_x \phi_x \right\rangle \left\langle \sum_y \phi_y \right\rangle \right].$$

In the following we shall regard $n_f T_r \ln(\mathcal{D} + m)$ as an external field term and treat it to lowest order in n_f .

Let us consider the Γ meson ($\Gamma = 1, \gamma_5, \dots$). We will write for its mass

$$m_\Gamma^2 = m_{\Gamma_0}^2 + n_f m_{\Gamma_1}^2 + O(n_f^2) \quad (6.3)$$

and its propagator in momentum space is given by

$$\frac{A_\Gamma}{p^2 + m_\Gamma^2} = \sum_x e^{ipx} \langle \bar{\psi}(x) \Gamma \psi(x) \bar{\psi}(0) \Gamma \psi(0) \rangle_U \quad (6.4)$$

with

$$A_\Gamma = A_{\Gamma_0} + n_f A_{\Gamma_1} + O(n_f^2). \quad (6.5)$$

To lowest order in n_f we then have

$$\begin{aligned} \frac{A_\Gamma}{p^2 + m_\Gamma^2} &= \frac{A_{\Gamma_0}}{p^2 + m_{\Gamma_0}^2} \\ &+ n_f \left[\frac{A_{\Gamma_1}}{p^2 + m_{\Gamma_0}^2} - \frac{A_{\Gamma_0} m_{\Gamma_1}^2}{(p^2 + m_{\Gamma_0}^2)^2} \right] \\ &+ O(n_f^2). \end{aligned} \quad (6.6)$$

In position space the terms $\propto n_f$ become

$$\begin{aligned} \frac{A_{\Gamma_1}}{2m_{\Gamma_0}} e^{-m_{\Gamma_0}|x|} \\ - \frac{A_{\Gamma_0} m_{\Gamma_1}^2}{4m_{\Gamma_0}^2} \left[\frac{1}{m_{\Gamma_0}} + |x| e^{-m_{\Gamma_0}|x|} \right] \end{aligned} \quad (6.7)$$

and in the pseudoscalar case the term proportional to $m_{\Gamma_0}^{-1}$ is dominant since $m_{\Gamma_0} \rightarrow 0$ when the quark mass is taken to zero. At zero external momentum we have

$$\frac{A_{\Gamma_0} m_{\Gamma_1}^2}{m_{\Gamma_0}^4} = \frac{1}{V} (\langle M_\Gamma^2 \rangle_U - \langle M_\Gamma \rangle_U^2) \quad (6.8)$$

with

$$M_\Gamma = \sum_x \bar{\psi}^{\cdot}(x) \Gamma \psi^{\cdot}(x), \quad (6.9)$$

where the superscript dots denote contraction. The symbol $\langle \cdot \rangle_U$ means average over gauge-field configurations whereas

$$\bar{\psi}^{\cdot}(x) \Gamma \psi^{\cdot}(x) = \text{tr}_{\text{spin color}} \Gamma(G, x, x; A). \quad (6.10)$$

Let us define a susceptibility χ_Γ associated with the state Γ ,

$$\chi_\Gamma = \frac{1}{V} (\langle M_\Gamma^2 \rangle_U - \langle M_\Gamma \rangle_U^2). \quad (6.11)$$

It is not a problem to compute it by Monte Carlo methods without having to include the effects of dynamic-fermion loops in the statistical factor. Then we have, for m_1 ,

$$m_1^2 = \frac{\chi_\Gamma m_{\Gamma_0}^4}{A_{\Gamma_0}}. \quad (6.12)$$

In terms of Feynman diagrams, m_1 contains the effects of correlations between two separate fermion loops at zero external momentum, with additional loops within the loops ignored. A_Γ is equal to γ_Γ^2 , which has been computed in the previous section for different values of β and small m . Let us now discuss the pseudoscalar case. In order to compute m_1 one has to determine χ_p for different values of m_0 and show that it diverges like m_0^{-4} .

We have tried to estimate m_1 in the pseudoscalar case at $\beta=5.6$ in the region $1.5 \lesssim m_\pi \lesssim 0.5$ using the Monte Carlo and the Langevin method on two gauge configurations with 6000–8000 pseudofermionic sweeps for each value of k on a $5 \times 5 \times 5 \times 8$ lattice. We find the following values

k	χ_p/A_{p0}	m_1	$m_1^2(m_V^2 - m_P^2)$
0.155	0.0030	0.09	0.029
0.16	0.0244	0.18	0.068
0.165	0.0942	0.21	0.090

(6.13)

Using the values for m_P and A_{Γ_0} listed in the tables

in the preceding sections and $a^{-1} \simeq 915$ MeV we find, indicatively,

$$m_1 \simeq 200 \pm 100 \text{ MeV}. \quad (6.14)$$

The η' mass can then be computed by diagonalizing the pseudoscalar mass matrix, with m_1 as off-diagonal matrix element, and using the relation

$$m_{\eta'}^2 = n_f m_1^2 - m_\eta^2 + 2m_K^2. \quad (6.15)$$

Experimentally one has $m_{\eta'} = 958$ MeV, whereas we find $m_\eta \simeq 300$ MeV and $m_{\eta'} \simeq 700$ MeV.

VII. CONCLUSION

We have shown in the preceding sections how reasonable estimates for the spectrum of QCD can be obtained in the approximation of neglecting dynamic-fermion loops.

A significant reduction in the statistical errors for the masses would require several orders of magnitude more computer time. At this level systematic effects associated with the smallness of the lattice, among others, will become important. Moreover, it becomes now crucial to investigate the effects of the inclusion of the fermion determinant into the measure factor. Work in this direction is in progress.

ACKNOWLEDGMENTS

The authors would like to thank members of the theory groups at Brookhaven and Rome, and in particular M. Creutz and C. Rebbi, for useful discussions, and the ISABELLE group and the Rome University INFN group for use of their VAX 11/780.

¹K. G. Wilson, Phys. Rev. D **10**, 2445 (1974); in *New Phenomena in Subnuclear Physics*, proceedings of the International School of Subnuclear Physics, Erice, 1975, edited by A. Zichichi (Plenum, New York 1977); and unpublished.

²H. Hamber and G. Parisi, Phys. Rev. Lett. **47**, 1795 (1981).

³E. Marinari, G. Parisi, and C. Rebbi, Phys. Rev. Lett. **47**, 1798 (1981).

⁴H. Hamber, E. Marinari, G. Parisi, and C. Rebbi, Phys. Lett. **B108**, 314 (1982).

⁵D. Weingarten, Phys. Lett. **B109**, 57 (1982). J. Kogut, S. Shenker, J. Shigemitsu, M. Stone, and H. Wyld, Phys. Rev. Lett. **48**, 1140 (1982).

⁶K. G. Wilson, in *Recent Developments in Gauge Theories*, proceedings of the NATO Advanced Study

Institute, Cargèse, 1979, edited by G. 't Hooft *et al.* (Plenum, New York, 1980); in *New Developments in Quantum Field Theory and Statistical Mechanics, Cargèse, 1976*, edited by M. Lévy and P. Mitter (Plenum, New York, 1977); M. Creutz, L. Jacobs, and C. Rebbi, Phys. Rev. Lett. **42**, 1390 (1979); Phys. Rev. D **20**, 1915 (1979); M. Creutz, Phys. Rev. Lett. **43**, 533 (1979); Phys. Rev. D **21**, 2308 (1980); Phys. Rev. Lett. **45**, 313 (1980); C. Rebbi, Phys. Rev. D **21**, 3350 (1980); G. Bhanot and C. Rebbi, Nucl. Phys. **180** [FS2], 469 (1981).

⁷F. Fucito, E. Marinari, G. Parisi, and C. Rebbi, Nucl. Phys. **B180** [FS2], 369 (1981).

⁸D. Scalapino and R. Sugar, Phys. Rev. Lett. **46**, 519 (1981).

⁹D. Weingarten and D. Petcher, Phys. Lett. **99B**, 33

- (1981).
- ¹⁰H. Hamber, Phys. Rev. D 14, 951 (1981).
- ¹¹A. Duncan and M. Furman, Nucl. Phys. B190 [FS3], 767 (1981).
- ¹²E. Marinari, G. Parisi, and C. Rebbi, Nucl. Phys. B190 [FS3], 734 (1981).
- ¹³R. Blankenbecler, D. J. Scalapino, and R. Sugar, Phys. Rev. D 14, 2278 (1981); D. J. Scalapino and R. Sugar, Phys. Rev. B 24, 4295 (1981); J. Hirsch, D. J. Scalapino, R. Sugar, and R. Blankenbecler, Phys. Rev. Lett. 47, 1628 (1981).
- ¹⁴J. Kuti, Phys. Rev. Lett. 49, 183 (1982).
- ¹⁵For a recent discussion of this point see E. Witten, Nucl. Phys. B156, 269 (1979), and references therein. See also P. Di Vecchia, K. Fabricius, G. C. Rossi, and G. Veneziano, Nucl. Phys. B192, 392 (1981).
- ¹⁶T. Banks, S. Raby, L. Susskind, J. Kogut, D. Jones, P. Scharbach, and D. Sinclair, Phys. Rev. D 15, 1111 (1977).
- ¹⁷L. Susskind, Phys. Rev. D 16, 3031 (1977).
- ¹⁸S. Drell, H. Quinn, B. Svetitsky, and M. Weinstein, Phys. Rev. D 22, 490 (1980); 22, 1190 (1980).
- ¹⁹N. Kawamoto, Nucl. Phys. B190 [FS3], 617 (1981).
- ²⁰N. Kawamoto and J. Smit, Nucl. Phys. B192, 10 (1981), and references therein.
- ²¹J. Hoek, N. Kawamoto, and J. Smit, Nucl. Phys. B199, 495 (1982).
- ²²H. Klugberg-Stern, A. Morel, O. Napoly, and B. Peterson, Nucl. Phys. B190 [FS3], 50 (1981); Saclay report, 1982 (unpublished).
- ²³P. Ginsparg and K. G. Wilson, Phys. Rev. D 25, 2649 (1982).
- ²⁴G. Parisi, Nucl. Phys. B180 [FS2], 378 (1981); B205 [FS5], 337 (1982); F. Fucito and E. Marinari, Nucl. Phys. B190, 266 (1981).
- ²⁵E. Pietarinen, Nucl. Phys. B190, 349 (1981).
- ²⁶A. Hasenfratz and P. Hasenfratz, Phys. Lett. 93B, 165 (1980).
- ²⁷C. Becchi, S. Narison, E. de Rafael, and F. J. Yundrian, Z. Phys. C 8, 335 (1981), and references therein.
- ²⁸A. Hasenfratz, P. Hasenfratz, Z. Kunszt, and C. Lang, Phys. Lett. 110B, 289 (1982).
- ²⁹F. Fucito, G. Martinelli, C. Omero, G. Parisi, P. Petronzio, and F. Rapuano, CERN report (in preparation).
- ³⁰S. Weinberg, in *Festschrift for I. Rabi*, edited by L. Motz (N.Y. Academy of Sciences, N.Y., 1977), p. 243.
- ³¹J. Richardson, Phys. Lett. 82B, 272 (1979).
- ³²G. Nagels *et al.*, Nucl. Phys. B147, 189 (1979).
- ³³R. Van Royen and V. Weisskopf, Nuovo Cimento 50, 617 (1967).